Coupled dynamics of electrons and phonons in metallic nanotubes:
Current saturation from hot-phonon generation

Michele Lazzeri and Francesco Mauri

Institut de Minéralogie et de Physique des Milieux Condensés, 4 Place Jussieu, 75252, Paris cedex 05, France

We show that the self-consistent dynamics of both phonons and electrons is the necessary ingredient for the reliable description of the hot phonons generation during electron transport in metallic single-wall carbon nanotubes (SWNTs). We solve the coupled Boltzmann transport equations to determine in a consistent way the current vs voltage (I-V) curve and the phonon occupation in metallic SWNTs which are lying on a substrate. We find a good agreement with measured I-V curves and we determine an optical phonon occupation which corresponds to an effective temperature of several thousands K (hot phonons), for the voltages typically used in experiments. We show that the high-bias resistivity strongly depends on the optical phonon thermalization time. This implies that a drastic improvement of metallic nanotubes performances can be achieved by increasing the coupling of the optical phonons with a thermalization source.

I. INTRODUCTION

Much interest is currently devoted to the study of electronic transport properties in carbon nanotubes (CNTs), both metallic and semiconducting. The main reason is the possibility of using CNTs in electronic integrated circuits thanks to catalizator-assisted on-site growth.[1,2] Semiconducting CNTs are forecast to become as new components for transistors and logic circuits.[3,4] On the other hand, metallic CNTs are particularly suited as a new type of interconnects due to their small dimensions and the large electron current density ($\sim 10^9$ A/cm^2) they can support. The current vs voltage (I-V) curve of metallic single-wall carbon nanotube (SWNTs) has been recently measured by several groups.[5–7] For voltages $\geqslant 0.2$ V, they observe a sudden increase of the resistivity which is due to the scattering with optical phonons (as already explained in Ref. 5). In long tubes, this leads to a saturation current of ~ 25 μA for voltages $\geqslant 5$ V. Such behavior limits the performance of metallic SWNTs as interconnects. The understanding of this phenomenon is, thus, a crucial step toward finding methods to boost SWNT performances and has important technological consequences.

Two recent papers[8,9] suggested the possibility that, at high bias, the electron transport induces an anomalously high optical-phonon occupation (hot phonons) which, in turn, induces an increase of the resistivity. In Ref. 8, this hypothesis is formulated on the basis of the comparison between scattering lengths (obtained from I-V measurements[5–7]) and electron-phonon coupling values (obtained from *ab initio* calculations[10] and inelastic x-ray scattering measurements[11]). However, the extent of Ref. 8 conclusions is limited, because Ref. 8 provides neither a scheme to reproduce experimental I-V curves, nor a reliable quantitative determination of the phonon occupation. The conclusions of Ref. 8 apply to tubes which are lying on a substrate. This is the very typical situation encountered in experiments.

Reference 9 reports the comparison between I-V curves measured on SWNTs in two different situations: when the tubes are lying on a substrate and when the tubes are sus-

pended between the two electrodes. Reference 9 concludes that hot phonons are present in the tubes which are suspended but are absent in those which are lying on a substrate (for bias <1 V). The presence of hot phonons is clearly demonstrated by the experimental observation of a negative differential resistance in suspended tubes. On the other hand, the absence of hot phonons is inferred from a simplified theoretical model in which the electron scattering length (at zero temperature) is a fitting parameter. The claim of absence of hot phonons for the tubes lying on a substrate contradicts the conclusions of Ref. 8, where the scattering length is obtained from *ab initio* calculations of the electron-phonon coupling.

A quantitative model to describe the anomalous phonon heating is not available. Moreover, given the contradictory conclusions of Refs. 8 and 9, it is not clear whether hot phonon generation is present for tubes lying on a substrate. This last point is particularly relevant. In fact, if the high-bias resistance measured for tubes lying on a substrate[5–7] is due to hot phonons,[8] one could conceive some methods to reduce the optical phonon temperature and thus diminish the high-bias resistance. This would not be possible if hot phonons were not present in tubes lying on a substrate.[9]

In this paper, we solve the coupled Boltzmann transport equations for both phonons and electrons to determine in a consistent way the IV curve and the phonon occupation in metallic SWNTs. The quantitative determination of the anomalous phonon heating during electron transport allows us to settle the debate on the presence/absence of hot phonons in nanotubes lying on a substrate. We are interested in the high bias (>0.2 V) region, where the transport properties are determined by the scattering with optical phonons. We use the zero-temperature electron scattering lengths obtained from *ab initio* calculations based on the density functional theory.[8,10,12]

II. DESCRIPTION OF THE MODEL

A. General considerations

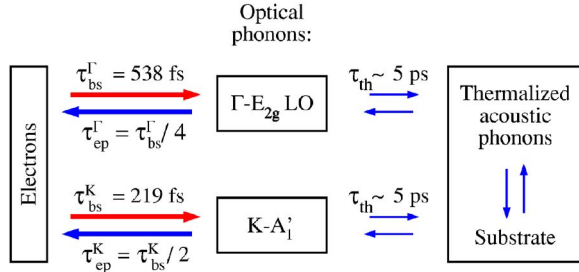In a metallic SWNT, there are only two phonons which can be generated by transport electrons via a backscattering

165419-1

FIG. 1. (Color online) Scheme of the model used in this paper.

process.[8] Using the graphene notation, they correspond to the E_{2g} LO (here LO stands for longitudinal along the tube axis) mode at $\mathbf{\Gamma}$ and to the A_1' mode at $\mathbf{K}$ (equivalent of the A_1' at $\mathbf{K'}$).[13] For simplicity, we label them $\mathbf{\Gamma}$ and $\mathbf{K}$; τ_{bs}^{Γ} and $\tau_{bs}^{\mathbf{K}}$ are the corresponding electron scattering times, i.e., the average time an electron can travel before emitting a phonon; $\tau_{bs} = l_{bs}/v_F$, where l_{bs} is the scattering length and $v_F = 8.39 \times 10^7$ cm/s is the Fermi velocity.[10] According to precise *ab initio* calculations,[8] at zero temperature $\tau_{bs}^{\Gamma} = 538$ and $\tau_{bs}^{\mathbf{K}} = 219$ fs[14] (for tubes with a diameter of 2.0 nm, which is the diameter typically used in experiments[5–7]).

Electron transport can induce not-thermal high-occupation of phonons if the generation time of the phonons (τ_{bs}^{Γ} and $\tau_{bs}^{\mathbf{K}}$) is shorter than their thermalization time. For metallic SWNTs, the optical-phonon thermalization time τ_{th} is due to anharmonic scattering into acoustic phonons.[15] Time-resolved terahertz spectroscopy measurements,[16] on graphite, reported an optical-phonon thermalization time of 7 ps. This value is comparable to the optical-phonon linewidth of diamond (the other carbon polymorph) ~ 1 cm^{-1}, which corresponds to a relaxation time of 5 ps, and is due to phonon-phonon scattering.[17] A τ_{th} value of the same order is also obtained by preliminary calculations of phonon-phonon scattering on graphite and nanotubes[18] done with the *ab initio* methods of Refs. 17 and 19. Concluding, we expect τ_{th} to be of the order of 5 ps. Since τ_{bs}^{Γ} and $\tau_{bs}^{\mathbf{K}}$ are much smaller than $\tau_{th} \sim 5$ ps, hot-phonon generation is *a priori* expected to occur during electron transport in metallic SWNTs.

In the following, we consider the model shown in Fig. 1. Transport electrons can scatter with the optical phonons $\mathbf{\Gamma}$, $\mathbf{K}$ and $\mathbf{K'}$ ($\mathbf{K'}$ is equivalent of $\mathbf{K}$ and is not shown). The terms τ_{bs}^{Γ} and $\tau_{bs}^{\mathbf{K}}$ are the electron scattering times; τ_{ep}^{Γ} and $\tau_{ep}^{\mathbf{K}}$ are phonon scattering times, i.e., the average time a phonon lives before emitting an electron-hole pair. For metallic SWNTs, it can be shown[20] that $\tau_{ep}^{\Gamma} = \tau_{bs}^{\Gamma}/4$ and $\tau_{ep}^{\mathbf{K}} = \tau_{bs}^{\mathbf{K}}/2$. The optical phonons can, also, scatter into acoustic phonons with a characteristic thermalization time $\tau_{th} \sim 5$ ps. In this model, both the acoustic phonons and the substrate are thermalized at room temperature, and are acting as a thermal bath. The present model is not valid if the tube is suspended between the two electrodes, as in some of the experiments of Ref. 9. In that case, the acoustic phonons are not thermalized with the environment and their occupation should be determined self-consistently. We are not considering that case.

B. Implementation

To study the evolution of the optical-phonons occupation during electron transport, we consider the Boltzmann trans-

port equation. In a metallic SWNT the electron gap is zero for two equivalent k points corresponding to $\mathbf{K}$ and $\mathbf{K'}$ in the graphite Brillouin zone. Two electron bands cross at the Fermi energy ϵ_F at both $\mathbf{K}$ and $\mathbf{K'}$. For the energy range of interest (± 0.5 eV around ϵ_F), the two bands can be considered linear with slope $\pm \hbar |v_F|$, where v_F is the Fermi velocity;[21] $f_{L/R}(k,x,t)$ is the probability to have an electron coming from the left or right contact (L,R) with momentum k ($k=0$ at the band crossing), at the position x. States near $\mathbf{K}$ or $\mathbf{K'}$ have the same distribution f; f evolves in time (t) according to

$$[\partial_t \pm v_F \partial_x - e\mathcal{E}/\hbar \ \partial_k] f_{L/R} = [\partial_t f_{L/R}]_c, \tag{1}$$

where v_F is the Fermi velocity and e ($e>0$) is the electron charge. For an applied voltage V, we consider a uniform electric field $\mathcal{E} = -V/L$, where L is the tube length. The collision term $[\partial_t f]_c$ describes the electron scattering. The probability distribution is given by the stationary solution of Eq. (1). As explained in Ref. 5, $[\partial_t f]_c$ can be considered as the sum of three terms: (1) the elastic scattering $[\partial_t f_L]_e = (v_F/l_e) \times (f_R - f_L)$, where l_e is the elastic scattering mean free path; (2) the forward scattering from optical phonons $[\partial_t f_L]_{fs}$; (3) the backscattering from optical phonons $[\partial_t f_L]_{bs}$. Following Refs. 7 and 9 we assume $l_e = 1600$ nm. We neglect $[\partial_t f_L]_{fs}$ since it does not change the propagation direction of electrons and, thus, should have a minor effect on the current. Now, we consider an optical phonon $\nu = \mathbf{\Gamma}, \mathbf{K}$, with occupation probability $n^\nu(k,x,t)$ (for the $\mathbf{K}$ phonon, k stands for $K+k$); n evolves according to

$$[\partial_t + v_{ph}^\nu(k)\partial_x]n^\nu = [\partial_t n^\nu]_c, \tag{2}$$

where v_{ph}^ν is the phonon velocity and $[\partial_t n^\nu]_c$ is the collision term. We use $v_{ph}^{\Gamma} = \text{sign}(k) \ 2.9 \times 10^5$ cm/s and $v_{ph}^{\mathbf{K}} = \text{sign}(k) \ 7.2 \times 10^5$ cm/s, from *ab initio* calculations,[10] where sign(k) is the sign of k. Given the small phonon velocity (with respect to v_F) the optical phonons do not have the time to diffuse along tubes longer than 100 nm (the thermalization scattering lengths are $l_{th}^{\Gamma} = v_{ph}^{\Gamma}\tau_{th} \sim 15$ nm and $l_{th}^{\mathbf{K}} = v_{ph}^{\mathbf{K}}\tau_{th} \sim 36$ nm). This was already pointed out in Ref. 9. Thus, the resulting IV curve is only slightly affected by the exact value of $|v_{ph}|$. For given x and t

$$[\partial_t f_L]_{bs} = \sum_\nu \frac{1}{\tau_{bs}^\nu} \{[1 - f_L]f_R(-k^+) - [1 - f_R(-k^-)]f_L$$

$$+ [f_R(-k^+) - f_L]n^\nu(-k-k^+)$$

$$+ [f_R(-k^-) - f_L]n^\nu(k+k^-)\} \tag{3}$$

$$[\partial_t n^\nu]_c = \frac{1}{2\tau_{ep}^\nu}\left\{\left[1 - f_L\left(\frac{-k^+}{2}\right)\right]f_R\left(\frac{k^-}{2}\right)\right.$$

$$+ \left[1 - f_R\left(\frac{-k^-}{2}\right)\right]f_L\left(\frac{k^+}{2}\right) \ + \ \left[-f_L\left(\frac{-k^+}{2}\right)\right.$$

$$\left.+ f_R\left(\frac{k^-}{2}\right) - f_R\left(\frac{-k^-}{2}\right) + f_L\left(\frac{k^+}{2}\right)\right]n^\nu(k)\right\} - \frac{1}{\tau_{th}}n^\nu(k), \tag{4}$$

where $k^\pm = k \pm (\omega^\nu/v_F)$, f_L stands for $f_L(k)$, the variables x and t are omitted, and $\nu = \mathbf{\Gamma}, \mathbf{K}$. The term ω^ν is the phonon pulsation, $\hbar\omega^{\mathbf{\Gamma}} = 196.0$ meV, $\hbar\omega^{\mathbf{K}} = 161.2$ meV and the ω^ν dependence on k can be neglected. Notice that Eq. (4) can be obtained from Eqs. (1)–(3), imposing the conservation of energy and momentum in the backscattering processes. The electron scattering times τ_{bs}^ν and τ_{ep}^ν of Eqs. (3) and (4) (Fig. 1) are obtained from the Fermi golden rule. The electron scattering times are usually written as depending on the phonon occupation [see, e.g., Eq. (1) of Ref. 8]. In the present case, the role of the phonon occupation is explicitly taken into account in the Boltzmann equation [Eqs. (3) and (4)]. Thus, to be consistent with the Boltzmann treatment, τ_{bs}^ν and τ_{ep}^ν are computed imposing zero phonon occupation.[14]

We impose the equilibrium distributions as boundary conditions

$$f_L(k,0) = f_R(-k,L) = \{\exp[\hbar v_F k/(k_B T)] + 1\}^{-1}$$

$$n^\nu(k > 0, 0) = n^\nu(k < 0, L) = 0,$$

where $T = 300$ K and k_B is the Boltzmann constant. The current is given by

$$I = \frac{4e}{h} \int (f_L - f_R) \hbar v_F dk.$$

The stationary solution of Eqs. (1) and (2) is found by numerical integration in time.[22]

The present approach is similar to that of Refs. 5 and 6 but has two important differences. First, in Refs. 5 and 6 the phonon occupation is considered to be thermalized at room temperature ($n \simeq 0$). Thus, in Refs. 5 and 6 Eq. (4) is not taken into account and, in Eq. (3), the terms depending on n are not considered. Second, in Refs. 5 and 6, the scattering time τ_{bs} is considered as a parameter and its value is fitted to reproduce the experimental I-V curves, supposing that hot phonons are absent. In the present work, we do not make any assumption on the phonon occupation n and we determine n by solving the transport equation. Moreover, the zero-temperature scattering times τ_{bs}^ν are not fitted to recover a better agreement with measurements, but are fixed to the values obtained from *ab initio* calculations.[8,10,12]

III. RESULTS

A. Current vs voltage

In Fig. 2 we show the comparison between the measured I-V curves and our calculations done imposing the phonon occupation $n = 0$ (cold phonons) or allowing the n to vary according to Eqs. (2)–(4), using $\tau_{th} = 5.31$ ps (hot phonons). This value corresponds to an anharmonic contribution to the phonon linewidth (full width) $\gamma = 1$ cm^{-1}, which is expected from independent calculations and measurements[16–18] (see discussion above). *Imposing $n = 0$ the resulting IV curve dramatically underestimates the experimental resistivity. On the contrary, if the phonon occupation n is determined self-consistently the I V curve nicely reproduces the experimental data.* Already at 0.2 V the hot-phonon and the cold-phonon curves significantly differ. This implies that the hot-phonon
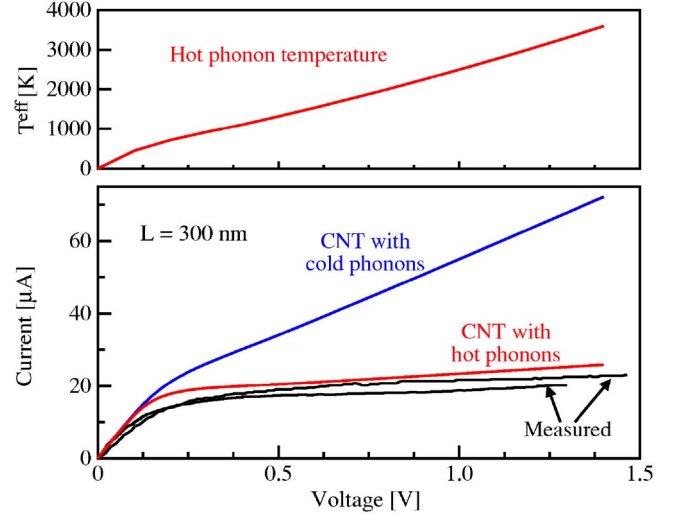

FIG. 2. (Color online) Lower panel: current vs voltage characteristic of a 300-nm-long carbon nanotube (CNT). Calculations are done fixing the phonon occupation to zero (cold phonons) or allowing phonons to heat up (hot phonons, $\tau_{th} = 5.31$ ps). Measurements are from Refs. 6 and 7. Upper panel: phonon effective temperature of the Raman G peak as a function of the voltage.

generation dominates the resistivity behavior already at $V > 0.2$ V, also for tubes lying on a substrate.

In Fig. 3 we show our calculations for tubes with different lengths L. The dependence of the I-V curve on L is similar to that observed experimentally in Refs. 6 and 7. Despite the presence of the hot phonons, for bias > 0.5 V the differential resistance dV/dI is almost independent from the voltage.

We computed the dV/dI at high bias (in between 1.0 and 1.4 V) for tubes with different lengths L (Fig. 4). Beside $\tau_{th} = 5.31$ ($\gamma = 1$ cm^{-1}), we also considered $\tau_{th} = 2.65$, 0.885, and 0 ps (corresponding to $\gamma = 2, 6, +\infty$ cm^{-1}), to investigate whether a significant reduction of the resistance can be achieved by a reduction of τ_{th}. dV/dI is clearly linear with respect to L and is, thus, possible to define a linear resistivity ρ. For a one-dimentional channel with four subbands, in the incoherent limit[23]
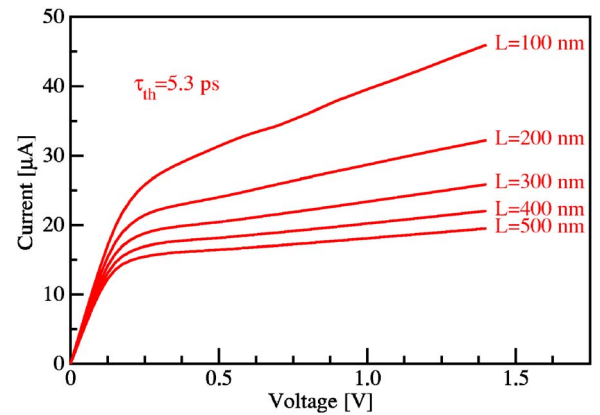

FIG. 3. (Color online) Current vs voltage curve calculated for various tube lengths (L); $\tau_{th} = 5.31$ ps.
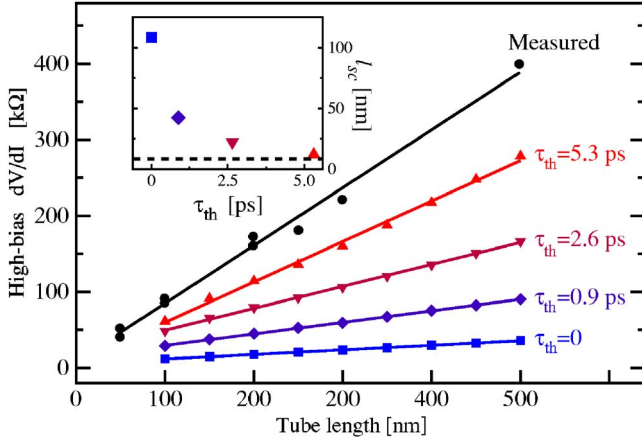
FIG. 4. (Color online) High-bias differential resistence for various tubes. Different symbols correspond to different τ_{th}. Measurements (dots) are from Ref. 7. Inset: the scattering length l_{sc} [defined in Eq. (5)] as a function of τ_{th}. The dashed line corresponds to the experimental value $l_{sc} = 8.5$ nm.

$$\rho = \frac{1}{L}\frac{dV}{dI} = \frac{1}{l_{sc}}\frac{h}{4e^2}, \tag{5}$$

where $h/(2e^2) = 12.9$ kΩ is the quantum of resistance and l_{sc} is the effective scattering length. Equation (5) can be used to obtain l_{sc} from the measured resistivity ρ. Using this approach, several independent experimental works[5–7,9] found a scattering length l_{sc} of the order of 10 nm, at high bias, for tubes lying on a substrate. We remark that l_{sc} is not to be confused with the l_{bs} of the present paper. While l_{bs} is calculated for zero phonon occupation, l_{sc} is an effective scattering length that includes the effects of the finite phonon occupation. To compare our calculations with the measured l_{sc}, we make a linear fit of the data in Fig. 4, we obtain ρ and, thus, l_{sc} through Eq. (5). This is done for the different τ_{th} values. For $\tau_{th} = 5.31$ ps (which is our best τ_{th} estimate) we obtain $l_{sc} = 12$ nm. Again, this compares very well with $l_{sc} = 8.5$ nm which we extracted from the experimental values[7] reported in Fig. 4.

Given the fact that the I-V curves strongly depend on the optical phonons occupation (Fig. 2), we expect that the thermalization time τ_{th} might play a crucial role. In fact, a smaller τ_{th} induces a lower optical phonons occupation (Fig. 1). In turn, this results in lower resistivity or a higher scattering length l_{sc}. Indeed, for $\tau_{th} = 2.65$, 0.885, and 0 ps, we obtain $l_{sc} = 22$, 42, and 108 nm, respectively (inset of Fig. 4). This strong dependence of l_{sc} on τ_{th} implies that even a small decrease of τ_{th} induces an important amelioration of the nanotube performances. A higher optical phonon thermalization can be obtained, e.g., by using a substrate characterized by vibrational frequencies similar to those of a CNT.[15] See also the related discussion in Ref. 24.

Finally, the calculations done with $\tau_{th} = 0$ are equivalent of imposing $n^\nu = 0$ (cold phonons) in Eqs. (3) and (4). For $n = 0$, it is usually assumed that l_{sc} is a measure of the optical phonon backscattering length, i.e., $(l_{sc})^{-1} = (l_{bs}^{\Gamma})^{-1} + (l_{bs}^{K})^{-1}$.
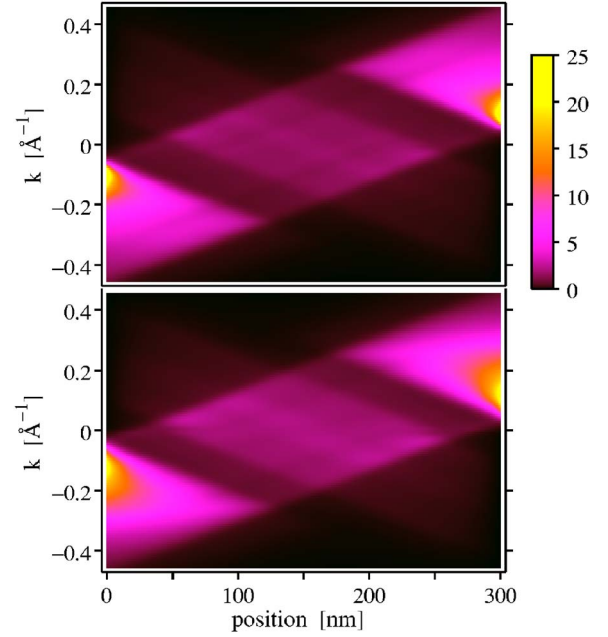

FIG. 5. (Color online) Phonon occupation n as a function of the position along the tube, x, and momentum k. Upper panel: Γ-E$_{2g}$ LO phonon. Lower panel: K-A$_1'$. The tube is the same as in Fig. 2, with voltage 1.4 V.

Indeed, from our calculations for $n = 0$ ($\tau_{th} = 0$) $l_{sc} = 108$ nm, which is 20% smaller than $[(l_{bs}^{\Gamma})^{-1} + (l_{bs}^{K})^{-1}]^{-1} = 131$ nm.

B. Phonon occupation

In Fig. 5, we show an example of the computed phonon occupation $n(k,x)$ at 1.4 V, $L = 300$ nm. The phonon occupation is clearly distributed not in a uniform way. Two important peaks with $n \sim 20$ are present near the electrodes. For a given phonon occupation $n(k,x)$, we define an effective temperature $T^{eff}(k,x)$ as the corresponding temperature within the Bose-Einstein statistics: $n = 1/\{exp[\hbar\omega/(k_B T^{eff})] - 1\}$. The term $n \sim 20$ is extremely high and corresponds to $T^{eff} \sim 40\,000$ K. Using simple arguments, it can be shown that $n(k,x) \neq 0$ only for $|k| < 2Ve/(\hbar v_F)$. This region is small compared to the Brillouin zone of graphite.[25] Thus, the hot phonons are indeed concentrated around Γ and K. To evaluate the impact of the large phonon occupation on the nanotube stability, we compute the average kinetic energy (per carbon atom) associated the hot phonons as

$$E^{at} = \sum_\nu \frac{m^\nu \hbar \omega^\nu}{2\pi N^{at}} \int n^\nu(k,x)\,dk\,dx,$$

where N^{at} is the number of atoms in the tube, $m^\Gamma = 1$ and $m^K = 2$ (to take into account both K and K$'$). $E^{at}/k_B = 50.6$ K, at bias 1.4 V and $L = 300$ nm. Thus, the actual average kinetic energy per atom, associated with the hot phonons, is not particularly high despite the high values reached by the hot phonons distribution, $n^\nu(k,x)$. Indeed, only a small subset of optical phonons is heated in a limited region of the k space. Concluding, the presence of hot phonons having temperatures of several thousands K is com-

patible with the fact that the tubes are not melting during electron transport.

As suggested in Ref. 8, the occupation of the E_{2g} phonon at $k=0$, $n^{\Gamma}(0,x)$, is accessible experimentally using Raman spectroscopy. Indeed, this mode is responsible for the G peak observed in Raman spectroscopy.[26,27] The Stokes and anti-Stokes G peak intensities are proportional to $n^{\Gamma}(0,x)+1$ and $n^{\Gamma}(0,x)$, respectively. From the measured Stokes and anti-Stokes ratio one can extract $n^{\Gamma}(0,x)$ of a SWNT during electron transport. In the upper panel of Fig. 2 we show, as a function of the applied bias, the effective temperature T^{eff} of the Raman active E_{2g} phonon, obtained from the average over the tube length of $n^{\Gamma}(0,x)$. Already at 1.0 V, we find a $T^{eff}=2500$ K (Fig. 2), corresponding to $n=0.7$.

Finally, Refs. 8 and 9 built two oversimplified models to describe the hot-phonon generation. Both models are based on the assumption that there is a simple relation between the effective scattering length l_{sc}, the zero-temperature back-scattering length l_{bs}, and the average phonon occupation n

$$l_{sc} = \frac{l_{bs}}{2n+1} \qquad (6)$$

[see Eq. (10) of Ref. 8 and lines 4–12, page 2 of Ref. 9]. Although *a priori* reasonable, Eq. (6) is in contradiction with the observation that the differential resistance (and hence l_{sc}) is constant with the voltage at high bias (Fig. 3), while the phonon occupation n is increasing with the voltage (upper

panel of Fig. 2). Therefore Eq. (6) cannot be used to construct quantitative models for the description of hot phonons in metallic SWNTs. The high-bias linearity of the I-V curve, that is observed experimentally in tubes with $L<500$ nm, might have led Refs. 5–7 and 9 into neglecting hot-phonon effects for tubes lying on a substrate.

IV. CONCLUSIONS

In conclusion, the explicit and self-consistent dynamics of both of phonons and electrons is the necessary ingredient for the reliable description of the hot phonons generation during electron transport in metallic SWNTs. We find a remarkable agreement with the experimental I-V curves. We have shown that the hot phonon generation cannot be properly described using the simplified models reported in Refs. 8 and 9. We demonstrate the presence of hot phonons for voltages >0.2 V also for tubes which are lying on a substrate. We have shown that the high-bias resistance strongly depends on the thermalization time of the optical phonons. As a direct consequence, an important improvement of metallic nano-tubes performances is, in principle, possible by decreasing the optical-phonons thermalization time.

[1] J. Kong, H. T. Soh, A. M. Cassel, C. F. Quate, and H. Dai, Nature (London) **395**, 29 (1998).

[2] Y.-C. Tseng, P. Xuan, A. Javey, R. Malloy, Q. Wang, J. Bokor, and H. Dai, Nano Lett. **4**, 123 (2004).

[3] S. Tans, A. Verschueren, and C. Dekker, Nature (London) **393**, 49 (1998).

[4] V. Derycke, R. Martel, J. Appenzeller, and Ph. Avouris, Nano Lett. **1**, 453 (2001).

[5] Z. Yao, C. L. Kane, and C. Dekker, Phys. Rev. Lett. **84**, 2941 (2000).

[6] A. Javey, J. Guo, M. Paulsson, Q. Wang, D. Mann, M. Lundstrom, and H. Dai, Phys. Rev. Lett. **92**, 106804 (2004).

[7] J-Y. Park, S. Rosenblatt, Y. Yaish, V. Sazonova, H. Üstünel, S. Braig, T. A. Arias, P. W. Brouwer, and P. L. McEuen, Nano Lett. **4**, 517 (2004).

[8] M. Lazzeri, S. Piscanec, F. Mauri, A. C. Ferrari, and J. Robertson, Phys. Rev. Lett. **95**, 236802 (2005).

[9] E. Pop, D. Mann, J. Cao, Q. Wang, K. Goodson, and H. Dai, Phys. Rev. Lett. **95**, 155505 (2005).

[10] S. Piscanec, M. Lazzeri, F. Mauri, A. C. Ferrari, and J. Robertson, Phys. Rev. Lett. **93**, 185503 (2004).

[11] J. Maultzsch, S. Reich, C. Thomsen, H. Requardt, and P. Ordejon, Phys. Rev. Lett. **92**, 075501 (2004).

[12] S. Baroni, S. de Gironcoli, A. Dal Corso, and P. Giannozzi, Rev. Mod. Phys. **73**, 515 (2001).

[13] Because of the momentum conservation, only the phonons near Γ or $\mathbf{K}$ can be involved in a scattering process with electrons near the Fermi level. Moreover, the Γ-E_{2g} LO mode and the $\mathbf{K}$-A_1' are

the only phonons with a not negligible electron-phonon coupling[8] for backscattering events.

[14] Following Ref. 8, the scattering lengths are proportional to the tube diameter d, in particular $l_{bs}^{\Gamma}=225.5\,d$ for the Γ-E_{2g} LO mode and $l_{bs}^{\mathbf{K}}=91.9\,d$ and for the $\mathbf{K}$-A_1'. These values are computed using the Fermi golden rule, with zero phonon occupation. $\tau_{bs}^{\Gamma}=l_{bs}^{\Gamma}/v_F$ and $\tau_{bs}^{\mathbf{K}}=l_{bs}^{\mathbf{K}}/v_F$.

[15] In general, τ_{th} is also determined by the direct coupling of the SWNT optical phonons with the substrate. Such coupling is relevant when the optical phonon frequencies are similar to those of the substrate. In the typical experimental situation, we expect this coupling to be negligible because the nanotube is lying on a SiO_2 substrate. SiO_2 phonon frequencies are smaller than the SWNTs optical phonons frequencies.

[16] T. Kampfrath, L. Perfetti, F. Schapper, C. Frischkorn, and M. Wolf, Phys. Rev. Lett. **95**, 187403 (2005).

[17] G. Lang, K. Karch, M. Schmitt, P. Pavone, A. P. Mayer, R. K. Wehner, and D. Strauch, Phys. Rev. B **59**, 6182 (1999).

[18] N. Bonini, M. Lazzeri, F. Mauri, and N. Marzari (unpublished).

[19] A. Shukla, M. Calandra, M. d'Astuto, M. Lazzeri, F. Mauri, C. Bellin, M. Krisch, J. Karpinski, S. M. Kazakov, J. Jun, D. Daghero, and K. Parlinski, Phys. Rev. Lett. **90**, 095506 (2003).

[20] This result can be easily derived considering the lifetimes (of both electrons and phonons) as given by the Fermi golden rule. See: M. Lazzeri, S. Piscanec, F. Mauri, A. C. Ferrari, and J. Robertson, cond-mat/0508700 (unpublished).

[21] The hyperbolic bands above and below the two linear bands can be populated by electrons which are scattering from the linear

bands to the hyperbolic bands (by phonon scattering). This process is activated when the electric field accelerates the electron until the electron energy reaches the hyperbolic-band edge. The electron-phonon scattering within the linear bands reduces the electron energy and contrasts this process. Therefore, we expect this process to be present for higher voltages than those presently considered.

[22] The probabilities $f(k,x)$ and $n(k,x)$ are defined on a grid of points equally spaced by $\Delta k = 0.01$ eV/$(\hbar v_F)$ and Δx going from 0.2 to 1 nm, depending on the tube length; f was evolved in time according to Eq. (1) using a finite time step of $\Delta x / v_F$. The values of f and n, that are necessary for the next time step, are obtained via a third-order polynomial spline interpolation in the k coordinate.

[23] S. Datta, *Electronic Transport in Mesoscopic Systems* (Cambridge University Press, London, 1995).

[24] D. Mann, E. Pop, J. Cao, Q. Wang, K. Goodson, and H. Dai, J. Phys. Chem. B **110**, 1502 (2006).

[25] For the voltage $V = 1.4$ V (used in Fig. 2) $2Ve/(\hbar v_F) = 0.51$ Å^{-1}, which is to be compared with $2\pi/a = 2.55$ Å^{-1}, where a is the graphite lattice parameter.

[26] A. Jorio, A. G. Souza Filho, G. Dresselhaus, M. S. Dresselhaus, A. K. Swan, M. S. Ünlü, B. Goldberg, M. A. Pimenta, J. H. Hafner, C. M. Lieber, and R. Saito, Phys. Rev. B **65**, 155412 (2002).

[27] M. Oron-Carl, F. Hennrich, M. M. Kappes, H. v. Lohneysen, and R. Krupke, Nano Lett. **5**, 1761 (2005).